Research Article

Khalid K. Ali*, Mohamed S. Mohamed, Weam G. Alharbi, and Marwa Maneea

Innovative analysis to the time-fractional *q*-deformed tanh-Gordon equation *via* modified double Laplace transform method

https://doi.org/10.1515/phys-2024-0094
received July 12, 2024; accepted September 27, 2024

Abstract: In this study, we introduce an efficient analysis of a new equation, termed the time-fractional *q*-deformed tanh-Gordon equation (TGE), which is the fractional form of the *q*-deformed TGE that was recently introduced by Ali and Alharbi. This equation represents a significant advancement in the field of mathematical physics, which is due to its applications in many fields including superconductivity and fiber optics. It has many applications in condensed matter physics and in modeling physical systems that exhibit violated symmetries. We investigate the *q*-deformed TGE in fractional form using Caputo fractional derivative to capture non-local and memory effects, which means they can take into account the entire history of a function rather than just its current value. Notably, this equation has not been previously solved in fractional form, making our approach pioneering in its analysis. We solve this equation utilizing the modified double Laplace transform method, which is considered a semi-analytical technique that combines the double Laplace transform with Adomian polynomials to enable us to extract nonlinear terms. This method renowned for its efficacy in handling fractional differential equations; this is evident from the results obtained in the tables by comparing the analytical solution with the approximate solution we obtained, as well as by calculating the absolute error between them. We examine the existence and the uniqueness of the solution utilizing Schaefer's fixed-point theorem. Different graphs in 2D and 3D are presented to clarify the effect of different parameters on the behavior of the solution, specially the fractional operator and the deformation parameter *q*.

Keywords: fractional calculus, *q*-deformed tanh-Gordon equation, double Laplace transform method, Adomian polynomials, Schaefer's fixed-point theorem, existence and uniqueness analysis

1 Introduction

Fractional calculus, a branch of mathematical analysis that extends the concept of differentiation and integration to non-integer orders, has found wide-ranging applications across various fields [1]. In physics, fractional calculus offers insights into anomalous diffusion processes, where particles exhibit non-Gaussian behavior, as well as in modeling viscoelastic materials and describing complex dynamical systems [2–5]. Engineering disciplines benefit from fractional calculus in signal processing, control theory, and electromagnetics, where it aids in optimizing system performance and designing efficient filters and antennas as well as fluid and optics fields [6–9]. The biomedical domain utilizes fractional calculus to model physiological processes such as drug release kinetics, nerve conduction, and bioelectrical impedance analysis [10,11]. Moreover, fractional calculus has made significant contributions to economics and finance, enabling more accurate modeling of long-term memory processes in asset price fluctuations and improving risk management strategies [12,13]. Its versatility and applicability continue to inspire innovative solutions across diverse fields, driving progress and fostering interdisciplinary collaborations.

Differential equations are powerful mathematical tools that model a wide range of real-world physical phenomena, enabling us to describe and predict systems with numerous applications, from engineering and physics to biology and economics [14,15].

The *q*-deformed function, introduced by Arai [16], is incorporated in the dynamical system, system's symmetry

* **Corresponding author: Khalid K. Ali,** Mathematics Department, Faculty of Science, Al-Azhar University, Nasr-City, Cairo, Egypt, e-mail: khalidkaram2012@azhar.edu.eg
Mohamed S. Mohamed: Department of Mathematics, College of Science, Taif University, P.O. Box 11099, Taif, 21944, Saudi Arabia, e-mail: m.saaad@tu.edu.sa
Weam G. Alharbi: Department of Mathematics, Faculty of Science, University of Tabuk, Tabuk, 71491, Saudi Arabia, e-mail: wgalharbi@ut.edu.sa
Marwa Maneea: Faculty of Engineering, MTI University, Cairo, Egypt, e-mail: Marwa.Hana@eng.mti.edu.eg

is broken, and symmetry breaking happens when a dynamical system's symmetry is not visible in its ground state or equilibrium state. The q-deformed equations arise from the concept of q-deformation, which is a generalization of certain algebraic structures, such as quantum groups, Lie algebras, and associative algebras. These equations incorporate a deformation parameter q into their formulation, leading to nontrivial modifications to their properties compared to their classical counterparts. These equations appear in versions of physical systems, which describe the behavior of particles, fields, and interactions in systems with noncommutative geometry or quantum group symmetries. Examples include q-deformed Schrödinger equations [17,18], q-deformed Klein-Gordon equations [19], and q-deformed Sinh-Gordon equation [20–22] that has been modified several times and solved either in the integer-order or fractional-order form. Recently, Ali and Alharbi [23] introduced a new equation called q-deformed tanh-Gordon equation (TGE), which is considered as a generalization of q-deformed sinh-Gordon equation. They provided an analytical solution to it using G'/G method as well as a numerical solution using the finite difference method. In this study, our aim is to extend the q-deformed TGE and represent it in fractional form by incorporating the Caputo fractional derivative (CFD), aiming to find an approximate solution for this equation. The integer-order TGE as presented in the study by Ali and Alharbi [23] is in the form:

$$\frac{\partial^2 \mathcal{U}}{\partial \varkappa^2} - \frac{\partial^2 \mathcal{U}}{\partial t^2} = [\tanh_q \mathcal{U}(\varkappa, t)^{\varrho}]^{\mathcal{P}} (e^{\lambda \mathcal{U}(\varkappa,t)} + \beta q)^{\rho} - g, \quad t \geq 0, \quad 0 < q \leq 1, \tag{1}$$

where

$$\tanh_q(\mathcal{U}) = \frac{e^{\mathcal{U}} - q e^{-\mathcal{U}}}{e^{\mathcal{U}} + q e^{-\mathcal{U}}}, \tag{2}$$

and $\varrho, \lambda, \mathcal{P}, g$, and β are constants $\in \mathbb{R}$. As Eq. (1) represents a recently new equation, its solutions have been explored on limited occasions. It is worth noting that Eq. (1) has not yet been addressed or solved in a fractional context; hence, the focus of this research lies in presenting its solutions in fractional form, underscoring the significant role that fractional calculus plays across numerous scientific disciplines and clarifying the effect of fractional-order derivative on the solution behavior.

In this article, we will solve the time-fractional q-deformed TGE (TF q-deformed TGE) in the form:

$${}^{c}\mathcal{D}_t^{\Theta} \mathcal{U}(\varkappa, t) = \frac{\partial^2 \mathcal{U}}{\partial \varkappa^2} - [\tanh_q \mathcal{U}(\varkappa, t)^{\varrho}]^{\mathcal{P}} (e^{\lambda \mathcal{U}(\varkappa,t)} + \beta q)^{\rho} + g \tag{3}$$

constrained by the initial conditions:

$$\mathcal{U}(\varkappa, 0) = \mathcal{U}_0(\varkappa)$$
$$\mathcal{U}_t(\varkappa, 0) = \mathcal{U}_{0t}(\varkappa),$$

where ${}^{c}\mathcal{D}_t^{\Theta}$ is the CFG with respect to time, and Θ is the fractional-order derivative, $1 < \Theta \leq 2$. We motivate to solve Eq. (3) to combine the advantages of the q-deformed TGE with the benefits of using fractional calculus. It has many applications in condensed matter physics and modeling physical systems that exhibit violated symmetries. Violation of symmetries means deviation from standard symmetry properties. Standard symmetry leads to conservation laws, such as conservation of energy and momentum, when these symmetries are violated, it can indicate new physics or phenomena that are not captured by traditional models. The q-deformed TGE is used to model optical solitons in fiber optics, where light pulses can travel long distances without changing shape. It is useful in studying phase transitions in condensed matter systems; researchers can examine how systems behave as they transition between different phases, particularly in systems where standard symmetry properties are violated. The violation of symmetry allows for a richer understanding of fundamental interactions and behavior of particles in particle physics. We merge fractional derivative to capture non-local and memory effects, which means they can take into account the entire history of a function rather than just its current value, and we may predict what happened in the future, so using fractional derivative in forming equations that have physical applications is very useful.

We will solve Eq. (3) using the modified double Laplace transform method ($\mathcal{MDLTM}$). Utilizing the double Laplace transform method (DLTM) technique to solve fractional partial differential equations (FPDEs) presents a robust method for addressing intricate mathematical challenges. This approach entails the simultaneous transformation of both time and space variables, facilitating the conversion of fractional derivatives into simplified algebraic expressions; this reduction greatly simplifies the solution process. Adomian polynomials (APs) effectively decompose and manage nonlinear terms in the equation. APs coupled with double Laplace transforms are employed, resulting in a modified version known as $\mathcal{MDLTM}$. This strategy has garnered recognition for its efficacy in managing equations featuring fractional operators and *PDEs* with mixed derivatives such as $\mathcal{U}_{txx}$. For further elaboration and applications, see previous studies [24–27].

The structure of this article is as follows: in Section 2, we outline the basics of CFD, APs, and the DLTM. Section 3 discusses the existence and uniqueness of the solutions under study. Section 4 introduces the implementation framework of $\mathcal{MDLTM}$ utilizing the Caputo definition.

Section 5 presents the numerical outcomes for solving the TF q-deformed TGE. These results are visually depicted in Section 6. Finally, Section 7 offers concluding remarks on the findings of this study.

2 Basic definitions

2.1 Fractional derivatives

There exist several definitions of fractional derivatives such as Riemann–Liouville, Riesz, Hadmard, Caputo-Fabrizio, and many others, each with its own advantages. The majority of researchers in fractional calculus direct their attention toward studying the *CFD* because it is widely adopted for modeling real-world phenomena for two main reasons. First, the CFD is constrained since it yields zero when applied to a constant, ensuring boundedness. Second, it facilitates the representation of initial conditions using an integer-order derivative. It is crucial to highlight that Caputo's definition is applicable only to functions demonstrating differentiability [28,29].

Definition 2.1. [1] The Caputo derivative of Θ order is defined by

$$ {}^{C}\mathcal{D}_{\mathcal{U}}^{\Theta}\mathcal{F}(\mathcal{U}) = \begin{cases} \mathsf{J}^{\mathsf{k}-\Theta}\dfrac{\mathrm{d}^{\mathsf{k}}}{\mathrm{d}\mathcal{U}^{\mathsf{k}}}\mathcal{F}(\mathcal{U}), & \mathsf{k}-1 < \Theta < \mathsf{k}, \\ \dfrac{\mathrm{d}^{\mathsf{k}}}{\mathrm{d}\mathcal{U}^{\mathsf{k}}}\mathcal{F}(\mathcal{U}), & \Theta = \mathsf{k}, \end{cases} \tag{4} $$

where $\mathsf{J}^{\mathsf{k}-\Theta}$ represents the Riemann–Liouville fractional integral, which can be stated as

$$ \mathsf{J}^{\Theta}\mathcal{F}(\mathcal{U}) = \frac{1}{\Gamma(\Theta)}\int_{0}^{\mathcal{U}}(\mathcal{U}-Y)^{(\Theta-1)}\mathcal{F}(Y)\mathrm{d}Y, \quad \mathcal{U} > 0, \Theta \in R^{+}, \tag{5} $$

where R^{+} denotes all real positive numbers, and $\Gamma(.)$ is the known Gamma function. The operator J^{Θ} satisfies the following properties for $\alpha, \beta \geq -1$:

$$ \mathsf{J}^{\alpha}\mathsf{J}^{\beta}\mathcal{F}(\mathcal{U}) = \mathsf{J}^{\alpha+\beta}\mathcal{F}(\mathcal{U}), \tag{6} $$

$$ \mathsf{J}^{\alpha}\mathsf{J}^{\beta}\mathcal{F}(\mathcal{U}) = \mathsf{J}^{\beta}\mathsf{J}^{\alpha}\mathcal{F}(\mathcal{U}), \tag{7} $$

$$ \mathsf{J}^{\alpha}\mathcal{U}^{\upsilon} = \frac{\Gamma(\upsilon+1)}{\Gamma(\upsilon+1+\alpha)}\mathcal{U}^{\upsilon+\alpha}, \tag{8} $$

CFD satisfies the following properties:

$$ {}^{C}\mathcal{D}_{\mathcal{U}}^{\Theta}[\mathsf{J}^{\Theta}\mathcal{F}(\mathcal{U})] = \mathcal{F}(\mathcal{U}), \tag{9} $$

$$ \mathsf{J}^{\Theta}[{}^{C}\mathcal{D}_{\mathcal{U}}^{\Theta}\mathcal{F}(\mathcal{U})] = \mathcal{F}(\mathcal{U}) - \sum_{\imath=0}^{\mathsf{k}-1}\mathcal{F}^{\imath}(0)\frac{\mathcal{U}^{\imath}}{\imath!}, \mathcal{U} > 0, \tag{10} $$

$$ {}^{C}\mathcal{D}^{\Theta}\mathcal{U}^{\nu} = \begin{cases} 0, & \text{for } \nu < \Theta, \\ \dfrac{\Gamma(\nu+1)}{\Gamma(\nu+1-\Theta)}\mathcal{U}^{\nu-\Theta}, & \text{for } \nu \geq \Theta. \end{cases} \tag{11} $$

2.2 APs

The Adomian decomposition method based on establishing the unknown function $\mathcal{Y}$ in a form of series of decompositions:

$$ \mathcal{Y} = \sum_{\kappa=0}^{\infty}\mathcal{Y}_{\kappa}. \tag{12} $$

The components $\mathcal{Y}_{\kappa}$ are computed recursively. The nonlinear term $\mathsf{F}(\mathcal{Y})$, such as $\mathcal{Y}^2, \mathcal{Y}^3, \sin\mathcal{Y}$, and $e^{\mathcal{Y}}$ can be expressed by APs $\mathcal{A}_{\kappa}$ in the form:

$$ \mathsf{F}(\mathcal{Y}) = \sum_{\kappa=0}^{\infty}\mathcal{A}_{\kappa}(\mathcal{Y}_0, \mathcal{Y}_1, \ldots, \mathcal{Y}_{\kappa}). \tag{13} $$

APs are applicable across various forms of nonlinearity. Adomian initially introduced a technique for computing these polynomials in the study by Adomian and Rach [30], a method later supported by formal validations. Additional methods have surfaced, including those based on Taylor series and similar techniques, as discussed in previous studies [31,32].

The calculation of APs, denoted as $\mathcal{A}_{\kappa}$, for the nonlinear component $\mathsf{F}(\mathcal{Y})$, can be accomplished using the general formula:

$$ \mathcal{A}_{\kappa} = \frac{1}{\kappa!}\frac{\mathrm{d}^{\kappa}}{\mathrm{d}\vee^{\kappa}}\left[\mathsf{F}\left(\sum_{\ell=0}^{\kappa}\vee^{\ell}\mathcal{Y}_{\ell}\right)\right]_{\vee=0}, \quad \kappa = 0, 1, 2, \ldots. \tag{14} $$

Eq. (14) can be expanded as

$$ \begin{aligned} \mathcal{A}_0 &= \mathsf{F}(\mathcal{Y}_0), \\ \mathcal{A}_1 &= \mathcal{Y}_1\mathsf{F}'(\mathcal{Y}_0), \\ \mathcal{A}_2 &= \mathcal{Y}_2\mathsf{F}'(\mathcal{Y}_0) + \frac{1}{2!}\mathcal{Y}_1^2\mathsf{F}''(\mathcal{Y}_0), \\ \mathcal{A}_3 &= \mathcal{Y}_3\mathsf{F}'(\mathcal{Y}_0) + \mathcal{Y}_1\mathcal{Y}_2F''(\mathcal{Y}_0) + \frac{1}{3!}\mathcal{Y}_1^3\mathsf{F}'''(\mathcal{Y}_0), \\ &\vdots \end{aligned} \tag{15} $$

From Eq. (15), we note that $\mathcal{A}_0$ depends only on $\mathcal{Y}_0$, $\mathcal{A}_1$ depends only on $\mathcal{Y}_0$, and $\mathcal{Y}_1$, and $\mathcal{A}_2$ depends only on $\mathcal{Y}_0$, $\mathcal{Y}_1$, and $\mathcal{Y}_2$.

2.3 Double Laplace transform method

The double Laplace transform method is a mathematical approach employed to solve fractional differential equations. It proves especially beneficial in tackling equations containing *CFD*, as it entails applying the Laplace transform twice, thereby converting a fractional differential equation into a more manageable algebraic form. This transformation aids in resolving fractional differential equations, particularly those featuring intricate fractional operators, especially when combined with APs to handle nonlinear terms [33].

Definition 2.2. Double Laplace transform in Caputo sense for $\mathsf{p} - 1 < \Theta \le \mathsf{p}$ is

$$\mathcal{L}_{\mathsf{x}}\mathcal{L}_{\mathsf{t}}\{{}^{C}\mathcal{D}_{\mathsf{x}}^{\Theta}\mathcal{F}(\mathsf{x},\mathsf{t})\} = \mathcal{S}_1^{\Theta}\mathcal{F}(\mathcal{S}_1,\mathcal{S}_2) - \sum_{\mathsf{i}=0}^{\mathsf{p}-1}\mathcal{S}_1^{\Theta-1-\mathsf{i}}\mathcal{L}_{\mathsf{t}}\left\{\frac{\partial^{\mathsf{i}}\mathcal{F}(0,\mathsf{t})}{\partial \mathsf{x}^{\mathsf{i}}}\right\}, \tag{16}$$

$$\mathcal{L}_{\mathsf{x}}\mathcal{L}_{\mathsf{t}}\{{}^{C}\mathcal{D}_{\mathsf{t}}^{\Theta}\mathcal{F}(\mathsf{x},\mathsf{t})\} = \mathcal{S}_2^{\Theta}\mathcal{F}(\mathcal{S}_1,\mathcal{S}_2) - \sum_{\mathsf{i}=0}^{\mathsf{p}-1}\mathcal{S}_2^{\Theta-1-\mathsf{i}}\mathcal{L}_{\mathsf{x}}\left\{\frac{\partial^{\mathsf{i}}\mathcal{F}(\mathsf{x},0)}{\partial \mathsf{t}^{\mathsf{i}}}\right\}. \tag{17}$$

3 Existence and uniqueness analysis

In this section, we will handle theoretical study about the TF q-deformed TGE including studying the existence and the uniqueness under *CFD*. Let us rewrite Eq. (3) in the form:

$${}^{c}\mathcal{D}_{\mathsf{t}}^{\Theta}\mathcal{U}(\varkappa,\mathsf{t}) = \Xi(\mathcal{U},\mathcal{U}_{\varkappa\varkappa}), 1 < \Theta \le 2, \tag{18}$$

subject to the initial constraints:

$$\mathcal{U}(\varkappa,0) = h(\varkappa),$$
$$\mathcal{U}_{\mathsf{t}}(\varkappa,0) = k(\varkappa).$$

To prove the uniqueness and the existence of the solution, let us consider the following important notations.

Definition 3.1. Consider a normed space denoted by $(U, \|.\|)$. A contraction on $\mathcal{U}$ refers to a mapping $\mathcal{M} : U \to U$ that fulfills the condition $\mathcal{U}_1, \mathcal{U}_2 \in U$.

$$\|\mathcal{M}(\mathcal{U}_1) - \mathcal{M}(\mathcal{U}_2)\| \le \varepsilon\|\mathcal{U}_1 - \mathcal{U}_2\|,$$

where ε is a real value $0 \le \varepsilon < 1$.

Theorem 3.2. [34] (Banach fixed point theorem) *Each contraction mapping within a complete metric space possesses a unique fixed point.*

Theorem 3.3. [35] (Schaefer–Krasnoselskii fixed point theorem) *Suppose U represents a convex subset of a closed and bounded Banach space $\mathcal{X}$, and let $\mathcal{M} : U \to U$ be a mapping that is completely continuous. In such a case, $\mathcal{M}$ necessarily possesses a fixed point within $\mathcal{M}$.*

Definition 3.4. Consider $C(\Omega, \mathcal{R})$ is a Banach space of all continuous functions from Ω to $\mathcal{R}$ with $\|.\|_\infty$ where $\|\mathcal{U}\|_\infty = \sup\{|\mathcal{U}|, (\varkappa,\mathsf{t}) \in \Omega\}$.

According to Eq. (18), suppose that the subsequent propositions hold:

p_1: There is a constant ϖ such that

$$|\mathcal{U}_{1\varkappa\varkappa} - \mathcal{U}_{2\varkappa\varkappa}| \le \varpi|\mathcal{U}_1 - \mathcal{U}_2|,$$

which is valid for all $(\varkappa,\mathsf{t}) \in \Omega$ and $\mathcal{U} \in C(\Omega,\mathcal{R})$.

p_2: There are constants θ_1 and θ_2 such that

$$|\Xi(\mathcal{U}_1,\mathcal{U}_{1\varkappa\varkappa}) - \Xi(\mathcal{U}_2,\mathcal{U}_{2\varkappa\varkappa})| \le \theta_1|\mathcal{U}_1 - \mathcal{U}_2| + \theta_2|\mathcal{U}_{1\varkappa\varkappa} - \mathcal{U}_{2\varkappa\varkappa}|,$$

which is valid for all $(\varkappa,\mathsf{t}) \in \Omega$ and $\mathcal{U} \in C(\Omega,\mathcal{R})$.

Theorem 3.5. *If the aforementioned propositions are hold, and if $\frac{\mathsf{t}^{\Theta}}{\Gamma(\Theta+1)}(\theta_1 + \varpi\theta_2) < 1$, in that case, the problem described in* Eq. (18) *possesses a unique solution.*

Proof. We intend to convert the problem stated in Eq. (18) into a fixed-point problem. Let us examine the operator:

$$\Lambda : C(\Omega,\mathcal{R}) \to C(\Omega,\mathcal{R}),$$

$$\Lambda(\mathcal{U}(\varkappa,\mathsf{t})) = h(\varkappa) + \mathsf{t}k(\varkappa) + \mathsf{J}_{\mathsf{t}}^{\Theta}(\Xi(\mathcal{U},\mathcal{U}_{\varkappa\varkappa})), 1 < \Theta \le 2.$$

It is obvious that the operator Λ is the solution of the problem under investigation. Now, we apply the Banach fixed-point theorem to demonstrate that the operator Λ possesses a fixed point. Let $\mathcal{U}_1, \mathcal{U}_1 \in C(\Omega,\mathcal{R})$, then for every $(\varkappa,\mathsf{t}) \in \Omega$:

$$\begin{aligned}
&|\Lambda\mathcal{U}_1(\varkappa,\mathsf{t}) - \Lambda\mathcal{U}_2(\varkappa,\mathsf{t})| \\
&= \mathsf{J}_{\mathsf{t}}^{\Theta}|\Xi(\mathcal{U}_1,\mathcal{U}_{1\varkappa\varkappa}) - \Xi(\mathcal{U}_2,\mathcal{U}_{2\varkappa\varkappa})| \\
&\le \mathsf{J}_{\mathsf{t}}^{\Theta}(\theta_1|\mathcal{U}_1 - \mathcal{U}_2| + \theta_2|\mathcal{U}_{1\varkappa\varkappa} - \mathcal{U}_{2\varkappa\varkappa}|) \\
&\le \mathsf{J}_{\mathsf{t}}^{\Theta}(\theta_1|\mathcal{U}_1 - \mathcal{U}_2| + \theta_2\varpi|\mathcal{U}_1 - \mathcal{U}_2|).
\end{aligned}$$

Hence,

$$\begin{aligned}
&|\Lambda\mathcal{U}_1(\varkappa,\mathsf{t}) - \Lambda\mathcal{U}_2(\varkappa,\mathsf{t})| \\
&\le \frac{\mathsf{t}^{\Theta}}{\Gamma(\Theta+1)}(\theta_1 + \theta_2\varpi)|\mathcal{U}_1 - \mathcal{U}_2| \\
&\le \frac{\mathsf{t}^{\Theta}}{\Gamma(\Theta+1)}(\theta_1 + \theta_2\varpi)\sup|\mathcal{U}_1 - \mathcal{U}_2| \\
&\le \frac{\mathsf{t}^{\Theta}}{\Gamma(\Theta+1)}(\theta_1 + \theta_2\varpi)\|\mathcal{U}_1 - \mathcal{U}_2\|_\infty.
\end{aligned}$$

Thus, according to the relation $\frac{t^{\Theta}}{\Gamma(\Theta+1)}(\theta_1+\varpi\theta_2)<1$, the operator Λ is identified as a contraction. As an immediate result of the Banach fixed-point theorem, it follows that Λ possesses a unique fixed point, which concludes the theorem's proof. □

Next, we establish the conditions that guarantee the existence of the solution utilizing Schaefer's fixed-point theorem.

Theorem 3.6. *If the following conditions are met, then, the equation presented in* (18) *possesses at least one solution within* $C(\Omega,\mathcal{R})$.

Suppose that $\mathcal{U}:\Omega\to\mathcal{R}$ *is continuous, and,*

Condition 1: *There is a constant* $\nu>0$ *in which*

$$|\Xi(\mathcal{U},\mathcal{U}_{\varkappa\varkappa})|\le\nu,\quad \text{for each } (\varkappa,t)\in\Omega \quad \text{and} \quad \mathcal{U}\in C(\Omega,\mathcal{R}).$$

Condition 2: *There are two constants* $\sigma_1,\sigma_2>0$ *in which*

$$\begin{aligned}|\Xi(\mathcal{U}(\varkappa_1,t_1),\mathcal{U}_{\varkappa\varkappa}(\varkappa_1,t_1))-\Xi(\mathcal{U}(\varkappa_2,t_2),\mathcal{U}_{\varkappa\varkappa}(\varkappa_2,t_2))|\\ \le\ \sigma_1|\mathcal{U}(\varkappa_1,t_1)-\mathcal{U}(\varkappa_2,t_2)|\\ +\sigma_2|\mathcal{U}_{\varkappa_1\varkappa_1}(\varkappa_1,t_1)-\mathcal{U}_{\varkappa_2\varkappa_2}(\varkappa_2,t_2)|,\end{aligned}$$

where $(\varkappa_1,t_1)$ *and* $(\varkappa_2,t_2)\in\Omega$, *and* $\mathcal{U}\in C(\Omega,\mathcal{R})$.

Condition 3: *There is a constant* $\wp>0$ *in which*

$$|\mathcal{U}_{\varkappa_1\varkappa_1}(\varkappa_1,t_1)-\mathcal{U}_{\varkappa_2\varkappa_2}(\varkappa_2,t_2)|\le\wp|\mathcal{U}(\varkappa_1,t_1)-\mathcal{U}(\varkappa_2,t_2)|,$$

for each $(\varkappa_1,t_1)$ *and* $(\varkappa_2,t_2)\in\Omega$, *and* $\mathcal{U}\in C(\Omega,\mathcal{R})$.

Condition 4: *There are two constants* $\ell_1,\ell_2>0$ *in which*

$$|\mathcal{U}(\varkappa_1,t_1)-\mathcal{U}(\varkappa_2,t_2)|\le\ell_1|\varkappa_1-\varkappa_2|+\ell_2|t_1-t_2|.$$

Proof. Suppose that $\mathcal{U}_m$ is a sequence converging to $\mathcal{U}$ in $C(\Omega,\mathcal{R})$, then, for each $(\varkappa,t)\Omega$, it holds that

$$|\Lambda\mathcal{U}_m(\varkappa,t)-\Lambda\mathcal{U}(\varkappa,t)|=J_t^{\Theta}|\Xi(\mathcal{U}_m,\mathcal{U}_{m\varkappa\varkappa})-\Xi(\mathcal{U},\mathcal{U}_{\varkappa\varkappa})|.$$

By utilizing the relation $\frac{t^{\Theta}}{\Gamma(\Theta+1)}(\theta_1+\varpi\theta_2)<1$, we have

$$|\Lambda\mathcal{U}_m(\varkappa,t)-\Lambda\mathcal{U}(\varkappa,t)|\le\frac{t^{\Theta}}{\Gamma(\Theta+1)}(\theta_1+\varpi\theta_2)\|\mathcal{U}_m-\mathcal{U}\|_{\infty}.$$

Since $\mathcal{U}$ is continuous, it follows that $\|\Lambda\mathcal{U}_m(\varkappa,t)-\Lambda\mathcal{U}(\varkappa,t)\|_{\infty}$ tends to *zero* as m tends to ∞.

Now, we want to prove that the mapping Λ maps bounded sets into bounded sets:

$$\begin{aligned}|\Lambda\mathcal{U}(\varkappa,t)|&=|h(\varkappa)+tk(\varkappa)+J_t^{\Theta}(\Xi(\mathcal{U},\mathcal{U}_{\varkappa\varkappa}))|\\ &\le|h(\varkappa)|+|tk(\varkappa)|+J_t^{\Theta}(\nu)\\ &\le|h(\varkappa)|+|tk(\varkappa)|+\frac{t^{\Theta}}{\Gamma(\Theta+1)}(\nu).\end{aligned}$$

Hence, $\|\Lambda\mathcal{U}(\varkappa,t)\|_{\infty}\le|h(\varkappa)|+|tk(\varkappa)|+\frac{t^{\Theta}}{\Gamma(\Theta+1)}(\nu)$, which means that $\|\Lambda\mathcal{U}(\varkappa,t)\|_{\infty}<\infty$. Next, we want to show that the mapping Λ is equicontinuous on $C(\Omega,\mathcal{R})$. To do that, let $(\varkappa_1,t_1),(\varkappa_2,t_2)\in\Omega$ and $\varkappa_1<\varkappa_2, t_1<t_2$, then

$$\begin{aligned}&|\Lambda\mathcal{U}(\varkappa_1,t_1)-\Lambda\mathcal{U}(\varkappa_2,t_2)|\\ &=J_t^{\Theta}|\Xi(\mathcal{U}(\varkappa_1,t_1),\mathcal{U}_{\varkappa_1\varkappa_1}(\varkappa_1,t_1))-\Xi(\mathcal{U}(\varkappa_2,t_2),\mathcal{U}_{\varkappa_2\varkappa_2}(\varkappa_2,t_2))|\\ &\le J_t^{\Theta}(\sigma_1|\mathcal{U}(\varkappa_1,t_1)-\mathcal{U}(\varkappa_2,t_2)|+\sigma_2|\mathcal{U}_{\varkappa_1\varkappa_1}(\varkappa_1,t_1)\\ &\quad-\mathcal{U}_{\varkappa_2\varkappa_2}(\varkappa_2,t_2)|)\\ &\le J_t^{\Theta}(\sigma_1|\mathcal{U}(\varkappa_1,t_1)-\mathcal{U}(\varkappa_2,t_2)|+\sigma_2\wp|\mathcal{U}(\varkappa_1,t_1)\\ &\quad-\mathcal{U}(\varkappa_2,t_2)|)\\ &\le\frac{t^{\Theta}}{\Gamma(\Theta+1)}((\sigma_1+\sigma_2\wp)(\ell_1|\varkappa_1-\varkappa_2|+\ell_2|t_1-t_2|))\\ &\le\frac{t^{\Theta}}{\Gamma(\Theta+1)}((\sigma_1+\sigma_2\wp)(\ell_1\|\varkappa_1-\varkappa_2\|_{\infty}+\ell_2\|t_1-t_2\|_{\infty})).\end{aligned}$$

In conclusion, we obtain

$$\begin{aligned}&|\Lambda\mathcal{U}(\varkappa_1,t_1)-\Lambda\mathcal{U}(\varkappa_2,t_2)|\\ &\le\frac{t^{\Theta}}{\Gamma(\Theta+1)}((\sigma_1+\sigma_2\wp)(\ell_1\|\varkappa_1-\varkappa_2\|_{\infty}+\ell_2\|t_1-t_2\|_{\infty})).\end{aligned}\tag{19}$$

The right-hand side of inequality (19) tends to *zero* as $\varkappa_1\longrightarrow\varkappa_2$ and $t_1\longrightarrow t_2$ and it is independent of $\mathcal{U}$, which implies that the mapping $\Lambda:(\Omega,\mathcal{R})\longrightarrow C(\Omega,\mathcal{R})$ is continuous and completely continuous.

As a result of Schaefer's fixed point theorem, we conclude that operator Λ possesses a fixed point, serving as a solution to the problem outlined in Eq. (18). □

4 Derivation of the TF q-deformed TGE using $\mathcal{MDLTM}$

For the following TF q-deformed TGE,

$$\begin{aligned}&{}^{c}\mathcal{D}_t^{\Theta}\mathcal{U}(\varkappa,t)\\ &\quad=\frac{\partial^2\mathcal{U}}{\partial\varkappa^2}-[\tanh_q\mathcal{U}(\varkappa,t)^{\varrho}]^{\mathcal{P}}\,(e^{\lambda\mathcal{U}(\varkappa,t)}+\beta q)^{\rho}+g.\end{aligned}\tag{20}$$

Eq. (20) will be handled in two cases according to the values of parameters $\varrho,\mathcal{P},\lambda,\beta,\rho$, and g.

Case I: For $\lambda=2,\varrho=\mathcal{P}=\beta=\rho=1$, and $g=-q$.

Using the relation presented in Eq. (2) with the values of parameters, (20) can be simplified into:

$${}^{c}\mathcal{D}_t^{\Theta}\mathcal{U}=\mathcal{U}_{\varkappa\varkappa}-e^{2\mathcal{U}},\quad 1<\Theta\le2,\tag{21}$$

constrained by

$$\mathcal{U}(\varkappa, 0) = \mathcal{U}_0(\varkappa),$$
$$\mathcal{U}_t(\varkappa, 0) = \mathcal{U}_{0t}(\varkappa).$$

Apply the Caputo double Laplace formula presented in Eq. (17) into both sides of Eq. (21), we obtain

$$\mathcal{L}_\varkappa\mathcal{L}_t\{{}^c\mathcal{D}_t^\Theta\mathcal{U}\} = \mathcal{L}_\varkappa\mathcal{L}_t\{\mathcal{U}_{\varkappa\varkappa}\} - \mathcal{L}_\varkappa\mathcal{L}_t\{e^{2\mathcal{U}}\}. \tag{22}$$

$$\begin{aligned}&\mathcal{S}^\Theta\mathcal{L}_\varkappa\mathcal{L}_t\{\mathcal{U}(\varkappa, t)\} - \mathcal{S}^{\Theta-1}\mathcal{L}_\varkappa\mathcal{U}(\varkappa, 0)\\ &\quad - \mathcal{S}^{\Theta-2}\mathcal{L}_\varkappa\mathcal{U}_t(\varkappa, 0) = \mathcal{L}_\varkappa\mathcal{L}_t\{\mathcal{U}_{\varkappa\varkappa}\} - \mathcal{L}_\varkappa\mathcal{L}_t\{e^{2\mathcal{U}}\}.\end{aligned} \tag{23}$$

Hence,

$$\begin{aligned}\mathcal{L}_\varkappa\mathcal{L}_t\{\mathcal{U}(\varkappa, t)\} = &\frac{1}{\mathcal{S}}\mathcal{L}_\varkappa\mathcal{U}(\varkappa, 0) + \frac{1}{\mathcal{S}^2}\mathcal{L}_\varkappa\mathcal{U}_t(\varkappa, 0)\\ &+ \frac{1}{\mathcal{S}^\Theta}\mathcal{L}_\varkappa\mathcal{L}_t\{\mathcal{U}_{\varkappa\varkappa}\} - \frac{1}{\mathcal{S}^\Theta}\mathcal{L}_\varkappa\mathcal{L}_t\{e^{2\mathcal{U}}\}.\end{aligned} \tag{24}$$

Apply *APs* to the nonlinear term $e^{2\mathcal{U}}$

$$\begin{aligned}&\mathsf{F}(\mathcal{U}) = e^{2\mathcal{U}},\\ &\mathscr{A}_0 = e^{2\mathcal{U}_0},\\ &\mathscr{A}_1 = 2\mathcal{U}_1e^{2\mathcal{U}_0},\\ &\mathscr{A}_2 = 2\mathcal{U}_2e^{2\mathcal{U}_0} + \frac{1}{2!}\mathcal{U}_1^2 4e^{2\mathcal{U}_0},\\ &\quad\vdots\end{aligned} \tag{25}$$

By applying inverse double Laplace transform into Eq. (24), we obtain the following sequence:

$$\begin{aligned}&\mathcal{U}_0 = \mathcal{U}(\varkappa, 0) + t\mathcal{U}_t(\varkappa, 0),\\ &\mathcal{U}_1 = \mathcal{L}_\varkappa^{-1}\mathcal{L}_t^{-1}\left\{\frac{1}{\mathcal{S}^\Theta}\mathcal{L}_\varkappa\mathcal{L}_t\left(\frac{\partial^2\mathcal{U}(\varkappa, 0)}{\partial\varkappa^2}\right)\right\}\\ &\qquad - \mathcal{L}_\varkappa^{-1}\mathcal{L}_t^{-1}\left\{\frac{1}{\mathcal{S}^\Theta}\mathcal{L}_\varkappa\mathcal{L}_t(\mathscr{A}_0)\right\}\\ &\mathcal{U}_2 = \mathcal{L}_\varkappa^{-1}\mathcal{L}_t^{-1}\left\{\frac{1}{\mathcal{S}^\Theta}\mathcal{L}_\varkappa\mathcal{L}_t\left(\frac{\partial^2\mathcal{U}_1}{\partial\varkappa^2}\right)\right\}\\ &\qquad - \mathcal{L}_\varkappa^{-1}\mathcal{L}_t^{-1}\left\{\frac{1}{\mathcal{S}^\Theta}\mathcal{L}_\varkappa\mathcal{L}_t(\mathscr{A}_1)\right\}\\ &\quad\vdots\end{aligned} \tag{26}$$

Finally, we can truncate at n term; hence, the approximated series solution will be in a series form:

$$\mathcal{U}(\varkappa, t) = \sum_{\mathfrak{p}=0}^{n}\mathcal{U}_\mathfrak{p}. \tag{27}$$

Case II: For $\varrho = \beta = 1$, $\lambda = \mathcal{P} = \rho = 2$, and $g = q^2$, Eq. (20) will be simplified into the form:

$${}^c\mathcal{D}_t^\Theta\mathcal{U} = \mathcal{U}_{\varkappa\varkappa} - e^{4\mathcal{U}} + 2qe^{2\mathcal{U}}, \quad 1 < \Theta \le 2. \tag{28}$$

Apply the same steps in Eqs. (22)–(24) to obtain the sequence of the solution:

$$\begin{aligned}&\mathcal{U}_0 = \mathcal{U}(\varkappa, 0) + t\mathcal{U}_t(\varkappa, 0),\\ &\mathcal{U}_1 = \mathcal{L}_\varkappa^{-1}\mathcal{L}_t^{-1}\left\{\frac{1}{\mathcal{S}^\Theta}\mathcal{L}_\varkappa\mathcal{L}_t\left(\frac{\partial^2\mathcal{U}_0}{\partial\varkappa^2}\right)\right\}\\ &\qquad - \mathcal{L}_\varkappa^{-1}\mathcal{L}_t^{-1}\left\{\frac{1}{\mathcal{S}^\Theta}\mathcal{L}_\varkappa\mathcal{L}_t(\mathscr{B}_0)\right\}\\ &\qquad + 2q\mathcal{L}_\varkappa^{-1}\mathcal{L}_t^{-1}\left\{\frac{1}{\mathcal{S}^\Theta}\mathcal{L}_\varkappa\mathcal{L}_t(\mathscr{N}_0)\right\}\\ &\mathcal{U}_2 = \mathcal{L}_\varkappa^{-1}\mathcal{L}_t^{-1}\left\{\frac{1}{\mathcal{S}^\Theta}\mathcal{L}_\varkappa\mathcal{L}_t\left(\frac{\partial^2\mathcal{U}_1}{\partial\varkappa^2}\right)\right\}\\ &\qquad - \mathcal{L}_\varkappa^{-1}\mathcal{L}_t^{-1}\left\{\frac{1}{\mathcal{S}^\Theta}\mathcal{L}_\varkappa\mathcal{L}_t(\mathscr{B}_0)\right\}\\ &\qquad + 2q\mathcal{L}_\varkappa^{-1}\mathcal{L}_t^{-1}\left\{\frac{1}{\mathcal{S}^\Theta}\mathcal{L}_\varkappa\mathcal{L}_t(\mathscr{N}_0)\right\}\\ &\quad:,\end{aligned} \tag{29}$$

where $\mathscr{B}_0, \mathscr{B}_1, \ldots$ are the *APs* of the function $\mathsf{F}(\mathcal{U}) = e^{4\mathcal{U}}$ and $\mathscr{N}_0, \mathscr{N}_1, \ldots$ are the *APs* of the function $\mathsf{F}(\mathcal{U}) = e^{2\mathcal{U}}$ represented as:

$$\begin{aligned}&\mathscr{B}_0 = e^{4\mathcal{U}_0}, \quad \mathscr{B}_1 = 4\mathcal{U}_1e^{4\mathcal{U}_0},\\ &\mathscr{N}_0 = e^{2\mathcal{U}_0}, \quad \text{and} \quad \mathscr{N}_1 = 2\mathcal{U}_1e^{2\mathcal{U}_0}.\end{aligned} \tag{30}$$

In the following, we conclude the steps of solving the nonlinear FPDE in a form of algorithm:

Step 1: Formulate the problem

Assume the TF differential equation in the form:

$${}^c\mathcal{D}_t^\Theta\mathcal{U} = L(\mathcal{U}) + N(\mathcal{U}), \quad 1 < \Theta \le 2, \tag{31}$$

constrained by

$$\mathcal{U}(\varkappa, 0) = \mathcal{U}_0(\varkappa) \quad \text{and} \quad \mathcal{U}_t(\varkappa, 0) = \mathcal{U}_{0t}(\varkappa),$$

where $L(\mathcal{U})$ and $N(\mathcal{U})$ are the linear and nonlinear terms, respectively.

Step 2: Apply the double Laplace transform

$$\mathcal{L}_\varkappa\mathcal{L}_t\{{}^c\mathcal{D}_t^\Theta\mathcal{U}\} = \mathcal{L}_\varkappa\mathcal{L}_t\{L(\mathcal{U})\} + \mathcal{L}_\varkappa\mathcal{L}_t\{N(\mathcal{U})\}. \tag{32}$$

Then, apply the initial constrains.

Step 3: Decompose the nonlinear terms

$$N(\mathcal{U}) = \sum_{\ell=0}^{\kappa}\mathscr{A}_\ell, \quad \kappa = 0, 1, 2, \ldots, \tag{33}$$

where $\mathscr{A}_\ell$ are the APs defined in Eq. (14).

Step 4: Inverse double Laplace

Apply the inverse double Laplace to Eq. (32) and put it in the form of successive approximations:

$$\begin{aligned}\mathcal{U}_{k+1}(\varkappa, t) = &\mathcal{L}_\varkappa^{-1}\mathcal{L}_t^{-1}\left\{\frac{1}{\mathcal{S}^\Theta}\mathcal{L}_\varkappa\mathcal{L}_t(L(\mathcal{U}_k))\right\}\\ &+ \mathcal{L}_\varkappa^{-1}\mathcal{L}_t^{-1}\left\{\frac{1}{\mathcal{S}^\Theta}\mathcal{L}_\varkappa\mathcal{L}_t(N(\mathcal{U}_k))\right\},\\ &k = 0, 1, 2, \ldots\end{aligned} \tag{34}$$

Step 5: Formulate the final approximate series solution

The final truncated series solution will be in the form:

$$\mathcal{U}(\varkappa, \mathrm{t}) = \sum_{k=0}^{n} \mathcal{U}_k, \tag{35}$$

where $\mathcal{U}_0 = \mathcal{U}(\varkappa, 0) + \mathrm{t}\mathcal{U}_{\mathrm{t}}(\varkappa, 0)$.

5 Application and numerical results for the proposed model

In this section, we present the numerical results of the two cases of the TF q-deformed TGE under CFD. We present our results supported by calculating the absolute error to confirm the accuracy of the obtained results.

Case I : Recall again the TF q-deformed TGE:

$${}^{c}\mathcal{D}_{\mathrm{t}}^{\Theta}\mathcal{U} = \mathcal{U}_{\varkappa\varkappa} - e^{2\mathcal{U}}, \quad 1 < \Theta \le 2, \tag{36}$$

constrained by

$$\mathcal{U}(\varkappa, 0) = \frac{1}{2}\ln\left[\mathcal{R}_0 + \mathcal{R}_1\left(\frac{\sqrt{\mathcal{E}^2 - 4\nu}\left(\mathcal{P}_2\cos\left(\frac{1}{2}(\mathcal{K}\varkappa)\sqrt{\mathcal{E}^2 - 4\nu}\right) - \mathcal{P}_1\sin\left(\frac{1}{2}(\mathcal{K}\varkappa)\sqrt{\mathcal{E}^2 - 4\nu}\right)\right)}{2\left(\mathcal{P}_1\cos\left(\frac{1}{2}(\mathcal{K}\varkappa)\sqrt{\mathcal{E}^2 - 4\nu}\right) + \mathcal{P}_2\sin\left(\frac{1}{2}(\mathcal{K}\varkappa)\sqrt{\mathcal{E}^2 - 4\nu}\right)\right)} - \frac{\mathcal{E}}{2}\right) + \mathcal{R}_2\left(\frac{\sqrt{\mathcal{E}^2 - 4\nu}\left(\mathcal{P}_2\cos\left(\frac{1}{2}(\mathcal{K}\varkappa)\sqrt{\mathcal{E}^2 - 4\nu}\right) - \mathcal{P}_1\sin\left(\frac{1}{2}(\mathcal{K}\varkappa)\sqrt{\mathcal{E}^2 - 4\nu}\right)\right)}{2\left(\mathcal{P}_1\cos\left(\frac{1}{2}(\mathcal{K}\varkappa)\sqrt{\mathcal{E}^2 - 4\nu}\right) + \mathcal{P}_2\sin\left(\frac{1}{2}(\mathcal{K}\varkappa)\sqrt{\mathcal{E}^2 - 4\nu}\right)\right)} - \frac{\mathcal{E}}{2}\right)^2\right],$$

$$\begin{aligned}\mathcal{U}_{\mathrm{t}}(\varkappa, 0) = {} & \vartheta(\mathcal{P}_1^2 + \mathcal{P}_2^2)\sqrt{\mathcal{E}^2 - 4\nu}\left(\mathcal{P}_1\sin\left(\frac{\varkappa\sqrt{\mathcal{E}^2 - 4\nu}\sqrt{\mathcal{R}_1 + \mathcal{E}\vartheta^2}}{2\sqrt{\mathcal{E}}}\right)\right. \\ & \left. - \mathcal{P}_2\cos\left(\frac{\varkappa\sqrt{\mathcal{E}^2 - 4\nu}\sqrt{\mathcal{R}_1 + \mathcal{E}\vartheta^2}}{2\sqrt{\mathcal{E}}}\right)\right) \Bigg/ \left[2\left(\mathcal{P}_1\cos\left(\frac{\varkappa\sqrt{\mathcal{E}^2 - 4\nu}\sqrt{\mathcal{R}_1 + \mathcal{E}\vartheta^2}}{2\sqrt{\mathcal{E}}}\right)\right.\right. \\ & \left. + \mathcal{P}_2\sin\left(\frac{\varkappa\sqrt{\mathcal{E}^2 - 4\nu}\sqrt{\mathcal{R}_1 + \mathcal{E}\vartheta^2}}{2\sqrt{\mathcal{E}}}\right)\right) + \left((\mathcal{P}_1^2 - \mathcal{P}_2^2)\cos\left(\frac{\varkappa\sqrt{\mathcal{E}^2 - 4\nu}\sqrt{\mathcal{R}_1 + \mathcal{E}\vartheta^2}}{\sqrt{\mathcal{E}}}\right)\right. \\ & \left.\left. + 2\mathcal{P}_1\mathcal{P}_2\sin\left(\frac{\varkappa\sqrt{\mathcal{E}^2 - 4\nu}\sqrt{\mathcal{R}_1 + \mathcal{E}\vartheta^2}}{\sqrt{\mathcal{E}}}\right)\right)\right],\end{aligned} \tag{37}$$

where $\mathcal{R}_0 = \frac{\mathcal{R}_1\nu}{\mathcal{E}}$, $\mathcal{R}_2 = \frac{\mathcal{R}_1}{\mathcal{E}}$, and $\mathcal{K} = \frac{\sqrt{\mathcal{R}_1 + \mathcal{E}\vartheta^2}}{\sqrt{\mathcal{E}}}$.

By substitution with the initial conditions on the solution sequence presented in Eq. (26), we obtain

$$\mathcal{U}_0 = \mathcal{U}(\varkappa, 0) + \mathrm{t}\mathcal{U}_{\mathrm{t}}(\varkappa, 0), \tag{38}$$

$$\begin{aligned}\mathcal{U}_1 = {} & -\frac{1}{\mathcal{E}\Gamma(\Theta)}\exp\left(\frac{\mathrm{t}\vartheta(\mathcal{P}_1^2 + \mathcal{P}_2^2)\sqrt{\mathcal{E}^2 - 4\nu}\left(\mathcal{P}_1\sin\left(\frac{\varkappa\sqrt{\mathcal{E}^2 - 4\nu}\sqrt{\mathcal{R}_1 + \mathcal{E}\vartheta^2}}{2\sqrt{\mathcal{E}}}\right)\right)}{\left(\mathcal{P}_1\cos\left(\frac{\varkappa\sqrt{\mathcal{E}^2 - 4\nu}\sqrt{\mathcal{R}_1 + \mathcal{E}\vartheta^2}}{2\sqrt{\mathcal{E}}}\right) + \mathcal{P}_2\sin\left(\frac{\varkappa\sqrt{\mathcal{E}^2 - 4\nu}\sqrt{\mathcal{R}_1 + \mathcal{E}\vartheta^2}}{2\sqrt{\mathcal{E}}}\right)\right)}\right) \\ & + \ldots \\ & + \mathcal{P}_2^3\mathcal{R}_1\mathcal{E}\vartheta\mathrm{t}^{\Theta+1}\sqrt{\mathcal{E}^2 - 4\nu}\cos\left(\frac{\varkappa\sqrt{\mathcal{E}^2 - 4\nu}\sqrt{\mathcal{R}_1 + \mathcal{E}\vartheta^2}}{2\sqrt{\mathcal{E}}}\right) \Bigg/ \\ & \times \left(8\Gamma(\Theta + 2)\left(\mathcal{P}_1\cos\left(\frac{\varkappa\sqrt{\mathcal{E}^2 - 4\nu}\sqrt{\mathcal{R}_1 + \mathcal{E}\vartheta^2}}{2\sqrt{\mathcal{E}}}\right)\right.\right. \\ & \left.\left. + \mathcal{P}_2\sin\left(\frac{\varkappa\sqrt{\mathcal{E}^2 - 4\nu}\sqrt{\mathcal{R}_1 + \mathcal{E}\vartheta^2}}{2\sqrt{\mathcal{E}}}\right)\right)\right) + \ldots.\end{aligned} \tag{39}$$

Using the procedure discussed in Section 4 and with the aid of Mathematica 13.2 program, we can calculate $\mathcal{U}_2, \mathcal{U}_3, \ldots$, but we stop at the second term because of the huge calculations; hence, the approximate series solution for case I is

$$\mathcal{U}(\varkappa, \mathrm{t}) = \mathcal{U}_0 + \mathcal{U}_1 + \mathcal{U}_2. \tag{40}$$

Table 1 provides the analytical results and the approximated results that we obtained and the absolute error at different values of $\varkappa$ for different time steps. One can note that the value of t exceeds, as the accuracy of the solution decreases, and this is normal behavior for all semi analytical solutions that possess an approximate series. The results we

Table 1: Comparison between analytical results in [23] and numerical values of $\mathcal{U}(\varkappa, \mathrm{t})$ presented in Eq. (40) and absolute error at $\mathcal{P}_1 = 0.1$, $\mathcal{P}_2 = 0.0001$, $v = 0.01$, $\mathcal{R}_1 = 0.001$, $\mathcal{E} = 0.001$, and $\vartheta = 0.4$ for $\Theta = 2$

	t = 0.01			t = 0.1			t = 0.2			t = 1
$\varkappa$	Analy.	Num.	Error	Analy.	Num.	Error	Analy.	Num.	Error	Error
–10	2.0590	2.0590	9.47×10^{-7}	2.0583	2.0584	9.47×10^{-5}	2.0576	2.0580	3.79×10^{-4}	9.50×10^{-3}
–6	2.1621	2.1621	7.39×10^{-7}	2.1611	2.1612	7.40×10^{-5}	2.1599	2.1602	2.96×10^{-4}	7.51×10^{-3}
–2	2.2805	2.2805	1.65×10^{-7}	2.2798	2.2798	1.66×10^{-5}	2.2790	2.2790	6.73×10^{-5}	1.82×10^{-3}
2	2.2806	2.2806	1.64×10^{-7}	2.2813	2.2813	1.63×10^{-5}	2.2821	2.2821	6.44×10^{-5}	1.46×10^{-3}
6	2.1624	2.1624	7.39×10^{-7}	2.1634	2.1635	7.37×10^{-5}	2.1646	2.1643	2.94×10^{-4}	7.27×10^{-3}
10	2.0591	2.0591	9.47×10^{-7}	2.0598	2.0599	9.47×10^{-5}	2.0605	2.0609	3.78×10^{-4}	9.44×10^{-3}

obtained illustrate the efficiency of the $\mathcal{MDLTM}$ in solving nonlinear FPDEs.

Case II : For the TF q-deformed TGE,

$$ {}^{c}\mathcal{D}_{\mathrm{t}}^{\Theta}\mathcal{U} = \mathcal{U}_{\varkappa\varkappa} - e^{4\mathcal{U}} + 2qe^{2\mathcal{U}}, \quad 1 < \Theta \le 2. \tag{41} $$

Subject to:

$$ \mathcal{U}(\varkappa, 0) = \ln\left(\mathcal{R}_0 + \left(\mathcal{R}_1\left(\frac{\sqrt{\mathcal{E}^2 - 4v}\left(\mathcal{P}_2\cos\left(\frac{1}{2}\mathcal{K}\varkappa\sqrt{\mathcal{E}^2 - 4v}\right) - \mathcal{P}_1\sin\left(\frac{1}{2}\mathcal{K}\varkappa\sqrt{\mathcal{E}^2 - 4v}\right)\right)}{2\left(\mathcal{P}_1\cos\left(\frac{1}{2}\mathcal{K}\varkappa\sqrt{\mathcal{E}^2 - 4v}\right) + \mathcal{P}_2\sin\left(\frac{1}{2}\mathcal{K}\varkappa\sqrt{\mathcal{E}^2 - 4v}\right)\right)} - \frac{\mathcal{E}}{2}\right)\right)^{0.5}\right), $$

$$ \begin{aligned} \mathcal{U}_{\mathrm{t}}(\varkappa, 0) = {} & -0.25\sqrt{q}\,\mathcal{E}(\mathcal{P}_1^2 + \mathcal{P}_2^2)(\mathcal{E}^2 - 4v)\sqrt{qv^2\left(\mathcal{K}^2 - \frac{8q^2}{\mathcal{E}^2 - 4v}\right)} \Big/ \left(v(0.5(\mathcal{P}_1^2 + \mathcal{P}_2^2)\sqrt{q^2\mathcal{E}^2(\mathcal{E}^2 - 4v)}\right. \\ & + 0.5(\mathcal{P}_1^2\sqrt{q^2\mathcal{E}^2(\mathcal{E}^2 - 4v)} + 2\mathcal{P}_1\mathcal{P}_2 q\mathcal{E}\sqrt{\mathcal{E}^2 - 4v} - \mathcal{P}_2^2\sqrt{q^2\mathcal{E}^2(\mathcal{E}^2 - 4v)})\cos(\mathcal{K}\varkappa\sqrt{\mathcal{E}^2 - 4v}) \\ & \left. - 0.5(\mathcal{P}_1^2 q\mathcal{E}\sqrt{\mathcal{E}^2 - 4v} - 2\mathcal{P}_1\mathcal{P}_2\sqrt{q^2\mathcal{E}^2(\mathcal{E}^2 - 4v)} - \mathcal{P}_2^2 q\mathcal{E}\sqrt{\sigma^2 - 4v})\sin(\mathcal{K}\varkappa\sqrt{\mathcal{E}^2 - 4v})\right)), \end{aligned} \tag{42} $$

where $\mathcal{R}_0 = \frac{q^2\mathcal{E}^2}{\sqrt{q^2\mathcal{E}^2(\mathcal{E}^2 - 4v)}} + q$, and $\mathcal{R}_1 = \frac{2q^2\mathcal{E}}{\sqrt{q^2\mathcal{E}^2(\mathcal{E}^2 - 4v)}}$.

By substitution with the initial conditions into the sequence (29), we obtain:

$$ \mathcal{U}_0 = \mathcal{U}(\varkappa, 0) + \mathrm{t}\mathcal{U}_{\mathrm{t}}(\varkappa, 0), \tag{43} $$

$$ \begin{aligned} \mathcal{U}_1 = {} & 0.5\mathcal{P}_2^4\mathcal{K}^2 q^2 v\mathrm{t}^{\Theta}\cos^4\left(\frac{1}{2}\mathcal{K}\varkappa\sqrt{\mathcal{E}^2 - 4v}\right) \Big/ \\ & \times \left(\left(\Gamma(\Theta + 1)\left(\mathcal{P}_1\cos\left(\frac{1}{2}\mathcal{K}\varkappa\sqrt{\mathcal{E}^2 - 4v}\right) + \mathcal{P}_2\sin\left(\frac{1}{2}\mathcal{K}\varkappa\sqrt{\mathcal{E}^2 - 4v}\right)\right)^4\right)\right. \\ & \times \left(\frac{2q^2\mathcal{E}\left(\frac{\sqrt{\mathcal{E}^2 - 4v}\left(\mathcal{P}_2\cos\left(\frac{1}{2}\mathcal{K}\varkappa\sqrt{\mathcal{E}^2 - 4v}\right) - \mathcal{P}_1\sin\left(\frac{1}{2}\mathcal{K}\varkappa\sqrt{\mathcal{E}^2 - 4v}\right)\right)}{2\left(\mathcal{P}_1\cos\left(\frac{1}{2}\mathcal{K}\varkappa\sqrt{\mathcal{E}^2 - 4v}\right) + \mathcal{P}_2\sin\left(\frac{1}{2}\mathcal{K}\varkappa\sqrt{\mathcal{E}^2 - 4v}\right)\right)} - \frac{\mathcal{E}}{2}\right)}{\sqrt{q^2\mathcal{E}^2(\mathcal{E}^2 - 4v)}} + \frac{q^2\mathcal{E}^2}{\sqrt{q^2\mathcal{E}^2(\mathcal{E}^2 - 4v)}} + q\right)^2\Bigg) \\ & + \ldots - \left(0.25\mathcal{P}_1\mathcal{P}_2^3\mathcal{K}^2\sqrt{q}\,\mathcal{E}^5\mathrm{t}^{\Theta+1}\sqrt{q^2\mathcal{E}^2(\mathcal{E}^2 - 4v)}\sqrt{qv^2\left(\mathcal{K}^2 - \frac{8q^2}{\mathcal{E}^2 - 4v}\right)}\sin(\mathcal{K}\varkappa\sqrt{\mathcal{E}^2 - 4v})\right) \Big/ \\ & \times (v\Gamma(\Theta + 2)(0.5(\mathcal{P}_1^2 + \mathcal{P}_2^2)\sqrt{q^2\mathcal{E}^2(\mathcal{E}^2 - 4v)} + 0.5(\mathcal{P}_1^2\sqrt{q^2\mathcal{E}^2(\mathcal{E}^2 - 4v)} + 2\mathcal{P}_1\mathcal{P}_2 q\mathcal{E}\sqrt{\mathcal{E}^2 - 4v} \\ & - \mathcal{P}_2^2\sqrt{q^2\mathcal{E}^2(\mathcal{E}^2 - 4v)})\cos(\mathcal{K}\varkappa\sqrt{\mathcal{E}^2 - 4v}) - 0.5(\mathcal{P}_1^2 q\mathcal{E}\sqrt{\mathcal{E}^2 - 4v} - 2\mathcal{P}_1\mathcal{P}_2\sqrt{q^2\mathcal{E}^2(\mathcal{E}^2 - 4v)} - \mathcal{P}_2^2 q\mathcal{E}\sqrt{\mathcal{E}^2 - 4v}) \\ & \times \sin(\mathcal{K}\varkappa\sqrt{\mathcal{E}^2 - 4v}))^2) + \ldots \end{aligned} \tag{44} $$

Table 2: Numerical results of the unknown function $\mathcal{U}(\varkappa, \mathrm{t})$ introduced in Eq. (45) compared with the analytical solution obtained in the study by Ali and Alharbi [23], and absolute error at $\mathcal{P}_1 = 0.4, \mathcal{P}_2 = 0.01, \nu = 0.1, \mathcal{K} = 0.3, \mathcal{E} = 0.001$, and $q = 0.001$ for $\Theta = 2$

	t = 0.01			t = 0.1			t = 0.2			t = 1
$\varkappa$	Analy.	Num.	Error	Analy.	Num.	Error	Analy.	Num.	Error	Error
–10	3.3561	3.3561	8.72×10^{-11}	3.3568	3.3568	8.40×10^{-9}	3.3577	3.3577	2.98×10^{-8}	2.46×10^{-6}
–6	3.3960	3.3960	6.20×10^{-11}	3.3970	3.3970	5.39×10^{-9}	3.3981	3.3981	1.19×10^{-8}	7.31×10^{-6}
–2	3.4349	3.4349	1.56×10^{-11}	3.4355	3.4355	2.61×10^{-9}	3.4361	3.4361	2.35×10^{-8}	1.22×10^{-5}
2	3.4348	3.4348	1.57×10^{-11}	3.4342	3.4342	2.64×10^{-9}	3.4335	3.4335	2.31×10^{-8}	9.41×10^{-6}
6	3.3958	3.3958	6.20×10^{-11}	3.3948	3.3948	5.45×10^{-9}	3.3936	3.3936	1.24×10^{-8}	7.16×10^{-6}
10	3.3559	3.3559	8.72×10^{-11}	3.3552	3.3552	8.43×10^{-9}	3.3544	3.3544	3.01×10^{-8}	1.95×10^{-6}

In this case, we can expand other terms, $\mathcal{U}_2, \mathcal{U}_3, \ldots$, but we stop at the second term; hence, the series that approximated the solution for case II is

$$\mathcal{U}(\varkappa, \mathrm{t}) = \mathcal{U}_0 + \mathcal{U}_1 + \mathcal{U}_2. \tag{45}$$

Table 2 represents the analytical solution and the numerical solution we obtained in (45) from solving the TF q-deformed TGE (case II) and the absolute error at $\mathcal{P}_1 = 0.4$, $\mathcal{P}_2 = 0.01$, $\nu = 0.1$, $\mathcal{K} = 0.3$, $\mathcal{E} = 0.001$, and $q = 0.001$ for $\Theta = 2$. From the table, we note that, the absolute error calculated by comparing the exact solution with the approximate solution obtained demonstrates the accuracy of the method used in the solution.

Table 3: Numerical results for the function $\mathcal{U}(\varkappa, \mathrm{t})$ introduced in Eq. (49), the analytical solution, and absolute error at $\mathcal{P}_1 = 0.3, \mathcal{P}_2 = 0.4, \nu = 0.001$, $\mathcal{K} = 0.4, \mathcal{E} = 0.1$, and $q = 0.4$ for $\Theta = 2$

	t = 0.01			t = 0.1			t = 0.2			t = 1
$\varkappa$	Analy.	Num.	Error	Analy.	Num.	Error	Analy.	Num.	Error	Error
–10	1.7663	1.7663	1.74×10^{-11}	1.7111	1.7111	2.19×10^{-7}	1.6516	1.6516	4.19×10^{-6}	2.32×10^{-3}
–6	1.8030	1.8030	1.27×10^{-11}	1.7504	1.7504	1.56×10^{-7}	1.6936	1.6936	2.94×10^{-6}	1.67×10^{-3}
–2	1.8410	1.8410	9.38×10^{-12}	1.7907	1.7907	1.12×10^{-7}	1.7364	1.7364	2.09×10^{-6}	1.21×10^{-3}
2	1.8803	1.8803	6.96×10^{-12}	1.8320	1.8320	8.23×10^{-8}	1.7799	1.7799	1.50×10^{-6}	8.83×10^{-4}
6	1.9206	1.9206	5.20×10^{-12}	1.8742	1.8742	6.06×10^{-8}	1.8241	1.8241	1.10×10^{-6}	6.48×10^{-4}
10	1.9620	1.9620	3.91×10^{-12}	1.9173	1.9173	4.50×10^{-8}	1.8689	1.8689	8.09×10^{-7}	4.79×10^{-4}

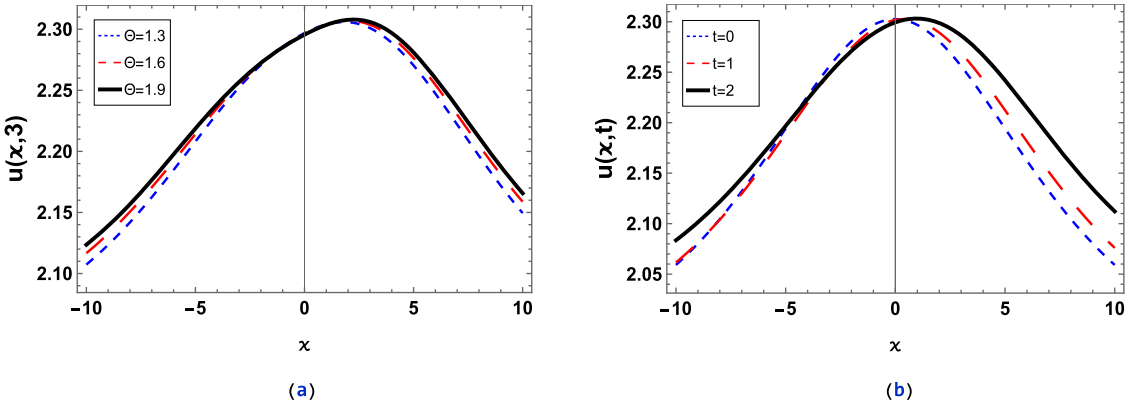

Figure 1: Approximate solution of TF q-deformed TGE (case I) presented in (40) using $\mathcal{MDLTM}$ at $\mathcal{P}_1 = 0.1, \mathcal{P}_2 = 0.0001, \nu = 0.01, \mathcal{R}_1 = 0.001$, $\mathcal{E} = 0.001$, and $\vartheta = 0.4$: (a) at $\mathrm{t} = 3$ for various values of Θ and (b) at $\Theta = 2$ for several steps of time.

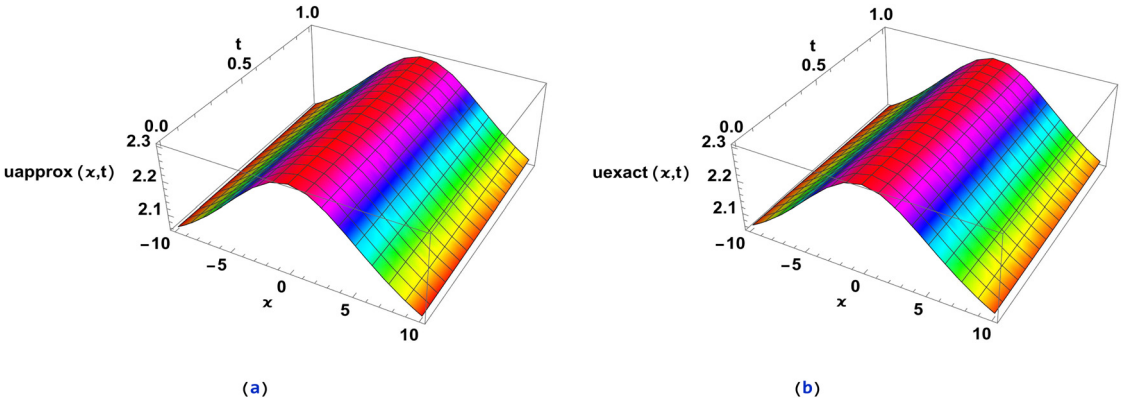

Figure 2: 3D representation of the solution of TF q-deformed TGE (case I) at $\mathcal{P}_1 = 0.1, \mathcal{P}_2 = 0.0001, \nu = 0.01, \mathcal{R}_1 = 0.001, \mathcal{E} = 0.001, \vartheta = 0.4$, and $\Theta = 2$. (a) The estimated solution presented in (40) and (b) the exact solution.

To study the effect of different parameters on the equation, especially the parameter q, we will solve the second case again, but under the influence of different initial conditions.

Case II under different initial condition: For the TF q-deformed TGE (41) constrained by

$$\mathcal{U}(\varkappa, 0) = \ln\left(\mathcal{R}_0 + \left(\mathcal{R}_1\left(\frac{\sqrt{\mathcal{E}^2 - 4\nu}\left(\mathcal{P}_1\sinh\left(\frac{1}{2}\mathcal{K}\varkappa\sqrt{\mathcal{E}^2 - 4\nu}\right) + \mathcal{P}_2\cosh\left(\frac{1}{2}\mathcal{K}\varkappa\sqrt{\mathcal{E}^2 - 4\nu}\right)\right)}{2\left(\mathcal{P}_1\cosh\left(\frac{1}{2}\mathcal{K}\varkappa\sqrt{\mathcal{E}^2 - 4\nu}\right) + \mathcal{P}_2\sinh\left(\frac{1}{2}\mathcal{K}\varkappa\sqrt{\mathcal{E}^2 - 4\nu}\right)\right)} - \frac{\mathcal{E}}{2}\right)^{0.5}\right)\right),$$

$$\begin{aligned}\mathcal{U}_t(\varkappa, 0) = &-(2\sqrt{q}\,\mathcal{E}(\mathcal{P}_1^2(\nu - 0.25\mathcal{E}^2) + \mathcal{P}_2^2(0.25\mathcal{E}^2 - \nu))\sqrt{q\nu^2\left(\mathcal{K}^2 - \frac{8q^2}{\mathcal{E}^2 - 4\nu}\right)}\Big) \Big/ (\nu(-(\mathcal{P}_1^2 - \mathcal{P}_2^2)\sqrt{q^2\mathcal{E}^2(\mathcal{E}^2 - 4\nu)}\\ &- (\mathcal{P}_1^2\sqrt{q^2\mathcal{E}^2(\mathcal{E}^2 - 4\nu)} - 2\mathcal{P}_1\mathcal{P}_2 q\mathcal{E}\sqrt{\mathcal{E}^2 - 4\nu} + \mathcal{P}_2^2\sqrt{q^2\mathcal{E}^2(\mathcal{E}^2 - 4\nu)})\cosh(\mathcal{K}\varkappa\sqrt{\mathcal{E}^2 - 4\nu})\\ &+ (\mathcal{P}_1^2 q\mathcal{E}\sqrt{\mathcal{E}^2 - 4\nu} + \mathcal{P}_2^2 q\mathcal{E}\sqrt{\mathcal{E}^2 - 4\nu} - 2\mathcal{P}_1\mathcal{P}_2\sqrt{q^2\mathcal{E}^2(\mathcal{E}^2 - 4\nu)})\sinh(\mathcal{K}\varkappa\sqrt{\mathcal{E}^2 - 4\nu})),\end{aligned} \tag{46}$$

where $\mathcal{R}_0 = q - \frac{q^2\mathcal{E}^2}{\sqrt{q^2\mathcal{E}^2(\mathcal{E}^2 - 4\nu)}}$, and $\mathcal{R}_1 = -\frac{2q^2\mathcal{E}}{\sqrt{q^2\mathcal{E}^2(\mathcal{E}^2 - 4\nu)}}$.

Substituting the initial conditions into the sequence (29), we obtain the sequence terms:

$$\mathcal{U}_0 = \mathcal{U}(\varkappa, 0) + t\mathcal{U}_t(\varkappa, 0), \tag{47}$$

$$\begin{aligned}\mathcal{U}_1 = &\left(0.5\mathcal{P}_2^4\mathcal{K}^2q^2\nu t^\Theta\cosh^4\left(\frac{1}{2}\mathcal{K}\varkappa\sqrt{\mathcal{E}^2 - 4\nu}\right)\right) \Big/ \left(\Gamma(\Theta + 1)\left(\mathcal{P}_1\cosh\left(\frac{1}{2}\mathcal{K}\varkappa\sqrt{\mathcal{E}^2 - 4\nu}\right) + \mathcal{P}_2\sinh\left(\frac{1}{2}\mathcal{K}\varkappa\sqrt{\mathcal{E}^2 - 4\nu}\right)\right)^4\right.\\ &*\left(-\frac{2q^2\mathcal{E}\left(\frac{\sqrt{\mathcal{E}^2 - 4\nu}\left(\mathcal{P}_1\sinh\left(\frac{1}{2}\mathcal{K}\varkappa\sqrt{\mathcal{E}^2 - 4\nu}\right) + \mathcal{P}_2\cosh\left(\frac{1}{2}\mathcal{K}\varkappa\sqrt{\mathcal{E}^2 - 4\nu}\right)\right)}{2\left(\mathcal{P}_1\cosh\left(\frac{1}{2}\mathcal{K}\varkappa\sqrt{\mathcal{E}^2 - 4\nu}\right) + \mathcal{P}_2\sinh\left(\frac{1}{2}\mathcal{K}\varkappa\sqrt{\mathcal{E}^2 - 4\nu}\right)\right)} - \frac{\mathcal{E}}{2}\right)}{\sqrt{q^2\mathcal{E}^2(\mathcal{E}^2 - 4\nu)}} - \frac{q^2\mathcal{E}^2}{\sqrt{q^2\mathcal{E}^2(\mathcal{E}^2 - 4\nu)}} + q\right)^2\Bigg)\\ &+\mathcal{P}_1^3\mathcal{P}_2\mathcal{K}^2\sqrt{q}\,\mathcal{E}^5t^{\Theta+1}\sqrt{q^2\mathcal{E}^2(\mathcal{E}^2 - 4\nu)}\sqrt{q\nu^2\left(\mathcal{K}^2 - \frac{8q^2}{\mathcal{E}^2 - 4\nu}\right)}\sinh(\mathcal{K}\varkappa\sqrt{\mathcal{E}^2 - 4\nu})/\\ &\times(\nu\Gamma(\Theta + 2)(-(\mathcal{P}_1^2 - \mathcal{P}_2^2)\sqrt{q^2\mathcal{E}^2(\mathcal{E}^2 - 4\nu)} - (\mathcal{P}_1^2\sqrt{q^2\mathcal{E}^2(\mathcal{E}^2 - 4\nu)} - 2\mathcal{P}_1\mathcal{P}_2 q\mathcal{E}\sqrt{\mathcal{E}^2 - 4\nu}\\ &+ \mathcal{P}_2^2\sqrt{q^2\mathcal{E}^2(\mathcal{E}^2 - 4\nu)})\cosh(\mathcal{K}\varkappa\sqrt{\mathcal{E}^2 - 4\nu})\\ &+ (\mathcal{P}_1^2 q\mathcal{E}\sqrt{\mathcal{E}^2 - 4\nu} - 2\mathcal{P}_1\mathcal{P}_2\sqrt{q^2\mathcal{E}^2(\mathcal{E}^2 - 4\nu)} + \mathcal{P}_2^2 q\mathcal{E}\sqrt{\mathcal{E}^2 - 4\nu})\sinh(\mathcal{K}\varkappa\sqrt{\mathcal{E}^2 - 4\nu}))^2) + \ldots\end{aligned} \tag{48}$$

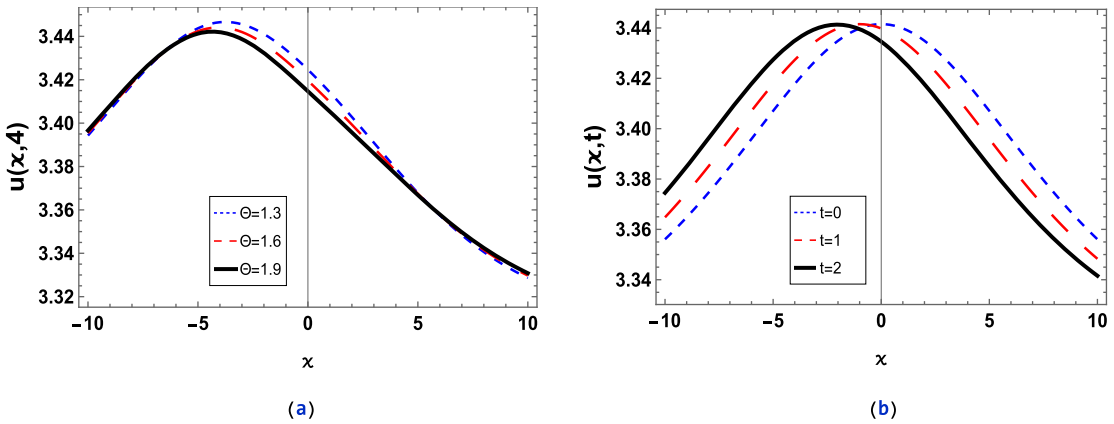

Figure 3: Approximate solution of TF q-deformed TGE (case II) presented in (45) using $\mathcal{MDLTM}$ at $\mathcal{P}_1 = 0.4, \mathcal{P}_2 = 0.01, \nu = 0.1, \mathcal{K} = 0.3, \mathcal{E} = 0.001$, and $q = 0.001$: (a) at t = 4 for various values of Θ and (b) at Θ = 2 for several stages of time.

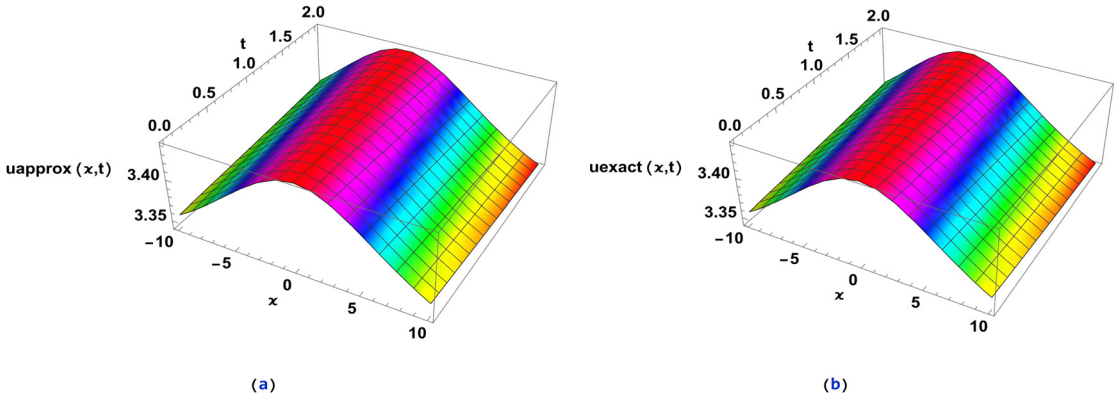

Figure 4: 3D representation of the solution of TF q-deformed TGE (case II) at $\mathcal{P}_1 = 0.4, \mathcal{P}_2 = 0.01, \nu = 0.1, \mathcal{K} = 0.3, \mathcal{E} = 0.001, q = 0.001$, and Θ = 2: (a) The estimated solution presented in (45) and (b) the exact solution.

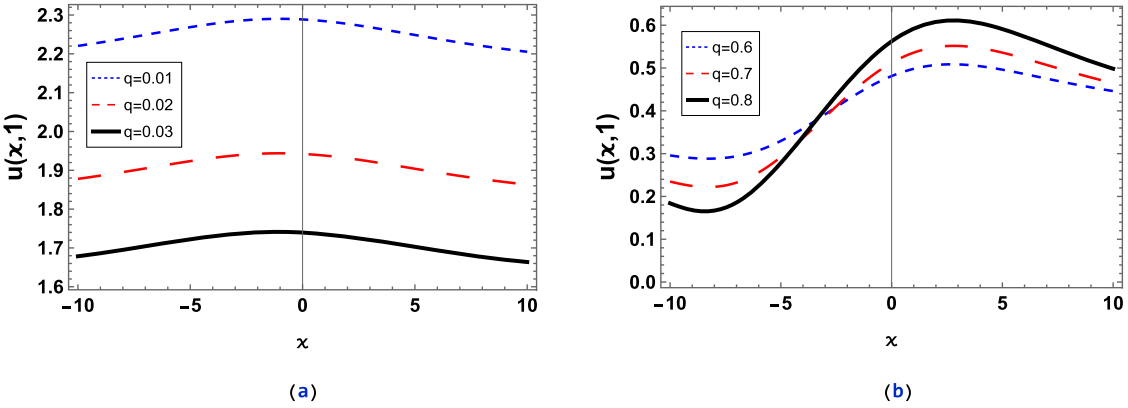

Figure 5: Approximate solution of TF q-deformed TGE (case II) presented in (45) at $\mathcal{P}_1 = 0.4, \mathcal{P}_2 = 0.01, \nu = 0.1, \mathcal{K} = 0.3, \mathcal{E} = 0.001$, t = 1, and Θ = 2. at different values of q.

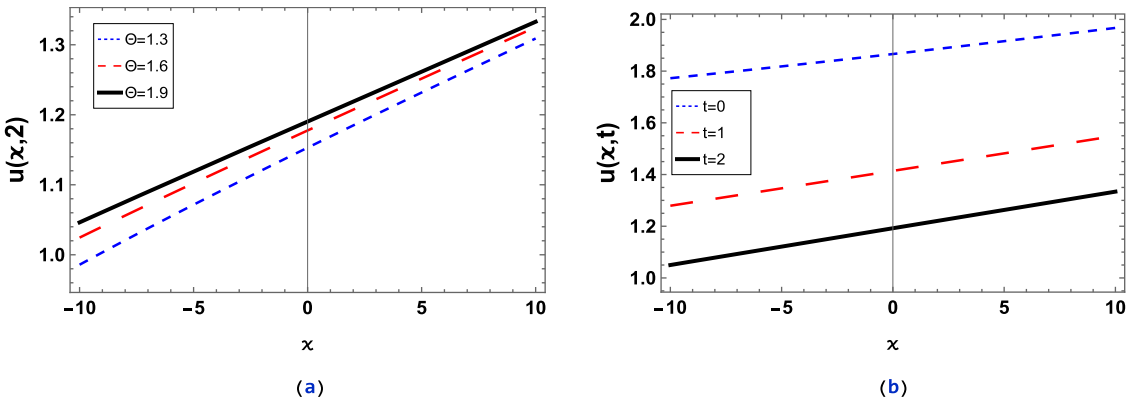

Figure 6: Estimated solution of TF q-deformed TGE (case II) presented in (49) at $\mathcal{P}_1 = 0.3$, $\mathcal{P}_2 = 0.4$, $v = 0.001$, $\mathcal{K} = 0.4$, $\mathcal{E} = 0.1$, and $q = 0.4$: (a) at t = 2 and (b) at Θ = 2 for distinct values of t.

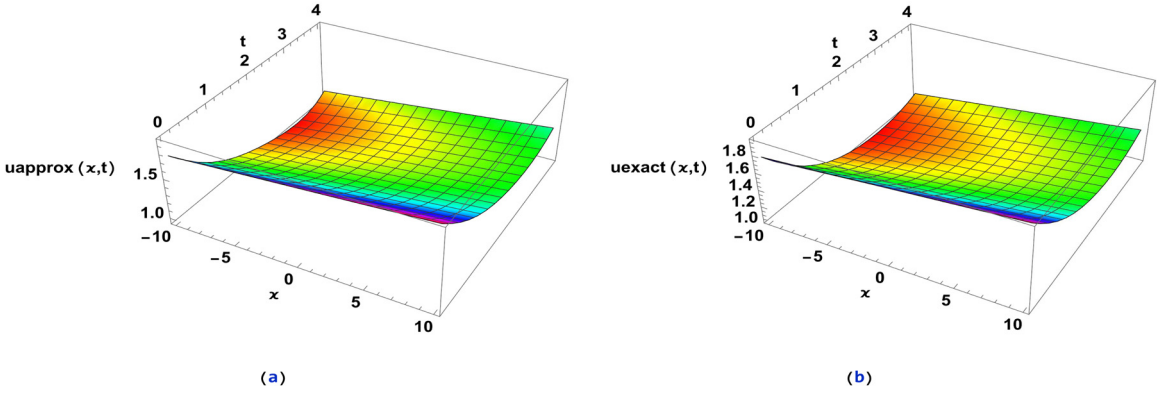

Figure 7: 3D representation of the solution of TF q-deformed TGE (case II) at $\mathcal{P}_1 = 0.3$, $\mathcal{P}_2 = 0.4$, $v = 0.001$, $\mathcal{K} = 0.4$, $\mathcal{E} = 0.1$, $q = 0.4$, and Θ = 2: (a) the estimated solution presented in (49) and (b) the exact solution.

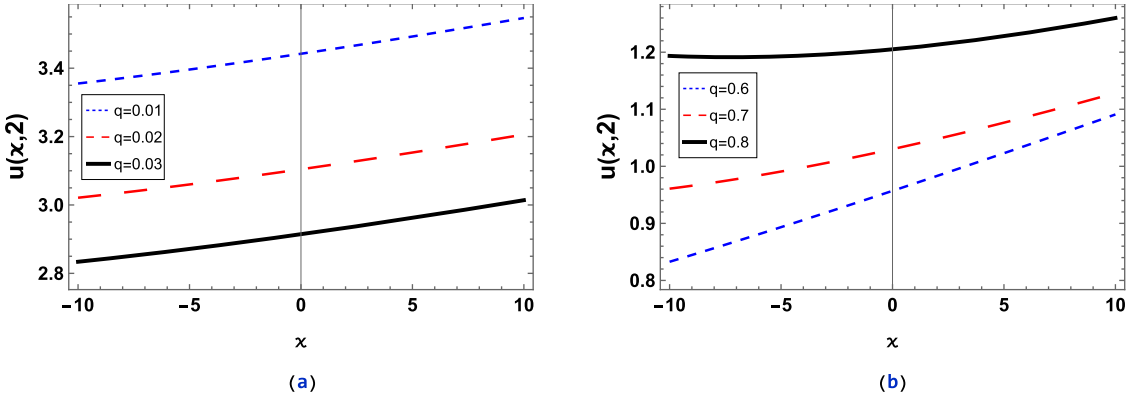

Figure 8: Estimated solution of TF q-deformed TGE (case II) presented in (49) at $\mathcal{P}_1 = 0.3$, $\mathcal{P}_2 = 0.4$, $v = 0.001$, $\mathcal{K} = 0.4$, $\mathcal{E} = 0.1$, t = 2, and Θ = 2. at various values of q.

As mentioned earlier, we can expand and compute $\mathcal{U}_2, \mathcal{U}_3, \ldots$ for the solution, but we will suffice due to the enormity of the computations; hence, the series that approximated the solution for case II using the second initial condition is

$$\mathcal{U}(\varkappa, \mathrm{t}) = \mathcal{U}_0 + \mathcal{U}_1 + \mathcal{U}_2. \tag{49}$$

Table 3 serves as a comprehensive tool for elucidating the analytical solutions outlined in the study of Ali and Alharbi [23] and showcasing the corresponding approximate values obtained in our study. These values were derived at various combinations of $\varkappa$ and t, while maintaining a fixed value of $\theta = 2$.

6 Visual representations

Visual representation, whether in two or three dimensions, offers an innovative means of illustrating the behavior of the studied model. These graphical representations facilitate a direct evaluation of the concurrence between the precise and approximated solutions, thereby allowing researchers to gauge the precision of the numerical technique utilized for generating the estimated solution. In this study, set of graphs in 2D and 3D were showcased in the context of solving the TF q-deformed TGE, contingent upon the initial conditions imposed on the model. Figure 1 illustrates the 2D depiction of the solution derived from the proposed model, considering initial conditions outlined in case I, Figure 1(a) at various fractional-order parameter values Θ with a constant time of $\mathrm{t} = 3$, and Figure 1(b) at $\Theta = 2$ across different time stages. In both cases, the solution is a soliton wave, and we observe that at time zero, the wave is symmetric, and as time increases, the wave moves to the right. Figure 2 represents the 3D configuration of case 1, Figure 2(a) clarifies the approximate solution that we obtained, and Figure 2(b) presents the analytical solution presented in [23], and the graphs are approximately consistent under the same conditions, which reflects the accuracy of the solutions we obtained. Figures 3 and 4 show the same representation in 2D and 3D for the solution of case II. Figure 5 represents the 2D wave solution using initial conditions in case I at fixed time $\mathrm{t} = 1$ and $\Theta = 2$ at different values of the deformation parameter q; this figure is very important because it clarifies the effect of q on the solution curves. Figure 5(a) presents the small values of q; in this case, decreasing q tends to dampen nonlinear effects in the equation, which can lead to smoother and more regular behavior in the solution, with less pronounced solitons and nonlinear waves. While increasing the values of q as presented in Figure 5(b) leads to stronger nonlinear effects in the equation, this can result in the amplification of soliton-like structures and nonlinear waves in the system. Figures 6–8 present the solution of the TF q-deformed TGE (case II) but under different initial conditions clarified in Eq. (46) to clarify the effect of the starting conditions on the behavior of solutions.

All graphs were plotted at the same parameter values provided in the study [23], which is considered the first study to introduce this equation, in order to obtain a comparative study to compare the results we obtained with the accurate results to demonstrate the accuracy of the results we obtained.

7 Conclusion

This study has introduced a novel equation called TF q-deformed TGE. This novel equation incorporates both fractional calculus and q-deformation, thereby offering a versatile framework for modeling physical systems characterized by violated symmetries. We solved this equation using a semi-analytical technique called $\mathcal{MDLTM}$ which is a combination between double Laplace transform method and APs. The results we obtained demonstrate the efficiency and high accuracy of the solutions, which is evident from the calculation of the absolute error shown in the tables pertaining to each case. We have explored the existence and uniqueness of the solution. Moreover, the presentation of various 2D and 3D graphs has offered insights into the influence of different parameters on the solution's behavior specially the effect of the fractional-order parameter, the deformation parameter, and the time; the 3D profile clarify great matches between the exact and the approximate solution, which reflects the validity of the technique we used.

For future directions, we aim to explore the TF q-deformed TGE in higher dimensions and find its solution using semi-analytical and numerical techniques. Moreover, examining the stability analysis of these solutions could pave the way for practical applications and simulations across various domains.

Acknowledgments: The authors extend their appreciation to Taif University, Saudi Arabia, for supporting this work through Project Number (TU-DSPP-2024-73).

Funding information: The authors extend their appreciation to Taif University, Saudi Arabia, for supporting this work through project number (TU-DSPP-2024-73).

Author contributions: All authors have accepted responsibility for the entire content of this manuscript and approved its submission.

Conflict of interest: The authors state no conflict of interest.

Data availability statement: All data generated or analysed during this study are included in this published article.

References

[1] Podlubny I. Fractional Differential Equations. San Diego: Academic Press; 1999.

[2] Elsaid A, Abdel Latif MS, Maneea M. Similarity solutions for multi-term time-fractional diffusion equation. Adv Math Phys. 2016;ID 7304659:7.

[3] Kulczycki P, Korbicz J, Kacprzyk J. Fractional dynamical systems: methods, algorithms and applications. Vol. 402. Switzerland: Springer; 2022.

[4] Hashemi MS, Ashpazzadeh E, Moharrami M, Lakestani M. Fractional order Alpert multiwavelets for discretizing delay fractional differential equation of pantograph type. Appl Numer Math. 2021;170:1–13.

[5] Li Z, Chen Q, Wang Y, Li X. Solving two-sided fractional super-diffusive partial differential equations with variable coefficients in a class of new reproducing kernel spaces. Fractal Fract. 2022;6:492.

[6] Lazarevic M. Advanced topics on applications of fractional calculus on control problems, system stability and modeling. Belgrade, Serbia: WSEAS Press; 2014.

[7] Biswal K, Swain S, Tripathy MC, Kar SK. Modeling and performance improvement of fractional-order band-pass filter using fractional elements. IETE J Res 2023;69(5):2791–800.

[8] Abu Arqub O. Numerical simulation of time-fractional partial differential equations arising in fluid flows via reproducing kernel method. Int J Numer Meth Heat Fluid Flow. 2020;30(11):4711–33.

[9] Mirzazadeh M, Hashemi MS, Akbulu A, Ur Rehman H, Iqbal I, Eslami M. Dynamics of optical solitons in the extended (3+1)-dimensional nonlinear conformable Kudryashov equation with generalized anti-cubic nonlinearity. Math Meth Appl Sci. 2024;47(7):5349–6737.

[10] Fan Z, Ali KK, Maneea M, Inc M, Yao S. Solution of time fractional Fitzhugh-Nagumo equation using semi analytical techniques. Results Phys. 2023;51:106679.

[11] Gao X, Zhang H, Li X. Research on pattern dynamics of a class of predator-prey model with interval biological coefficients for capture. AIMS Math. 2024;9(7):18506–27.

[12] Ali KK, Maaty MA, Maneea M. Optimizing option pricing: Exact and approximate solutions for the time-fractional Ivancevic model. Alexandr Eng J. 2023;84:59–70.

[13] Gao X, Li Z, Wang Y. Chaotic Dynamic Behavior of a Fractional-Order Financial System with Constant Inelastic Demand. Int J Bifurcat Chaos. 2024;34(9):2450111.

[14] Abu Arqub O. Computational algorithm for solving singular Fredholm time-fractional partial integro differential equations with error estimates. J Appl Math Comput. 2019;59:227–43.

[15] Hashemi MS. A variable coefficient third degree generalized Abel equation method for solving stochastic Schrödinger-Hirota model. Chaos Solitons Fractals. 2024;180:114606.

[16] Arai A. Exactly solvable supersymmetric quantum mechanics. J Math Anal Appl. 1991;158(1):63–79.

[17] Carow-Watamura U, Watamura S. The q-deformed Schrodinger Equation of The Harmonic Oscillator on the Quantum Euclidean Space. Int J Modern Phys A. 1994;9(22):3989–4008.

[18] Dobrogowska A, Odzijewicz A. Solutions of the q-deformed Schrödinger equation for special potentials. J Phys A Math Theoretic. 2007;40(9):2023.

[19] Lutfuoglu BC, Ikot AN, Chukwocha EO, Bazuaye FE. Analytical solution of the Klein Gordon equation with a multi-parameter q-deformed Woods-Saxon type potential. Europ Phys J Plus. 2018;133:528.

[20] Eleuch H. Some analytical solitary wave solutions for the generalized q-deformed sinh-Gordon equation: $\frac{\partial^2 u}{\partial z \partial \zeta} = e^{\Theta u}[sinh_q(u^\gamma)]^p \quad \delta$. Adv Math Phys. 2018;ID 5242757:7.

[21] Alrebdi HI, Raza N, Arshed S, Butt AR, Abdel-Aty A, Cesarano C, et al. A variety of new explicit analytical soliton solutions of q-deformed Sinh-Gordon in (2+1) dimensions. Symmetry. 2022;14:2425.

[22] Ali KK, Mohamed MS, Maneea M. Exploring optical soliton solutions of the time fractional q-deformed Sinh-Gordon equation using a semi-analytic method. AIMS Math. 2023;8(11):27947–68.

[23] Ali KK, Alharbi WG. Exploring unconventional optical soliton solutions for a novel q-deformed mathematical model. AIMS Math. 2024;9(6):22.

[24] Omran M, Kilicman A. Fractional double Laplace transform and its properties. AIP Confer Proc. 2017;1795:20021.

[25] Khan A, Khan TS, Syam MI, Khan H. Analytical solutions of time-fractional wave equation by double Laplace transform method. Europ Phys J Plus. 2019;134:163.

[26] Modanli M, Goktepe E, Akgul A, Alsallami SM, Khalil EM. Two approximation methods for fractional-order pseudo-parabolic differential equations. Alexandr Eng J. 2022;61:10333–9.

[27] Alsallami SAM, Maneea M, Khalil EM, Abdel-Khalek S, Ali KK. Insights into time fractional dynamics in the Belousov-Zhabotinsky system through singular and non-singular kernels. Scientif Reports. 2023;13:22347.

[28] Samko SG, Kilbas AA, Marichev OL. Fractional integrals and derivatives: theory and applications. New York: Gordon and Breach; 1993.

[29] Miller KS, Ross B. An Introduction to the Fractional Calculus and Fractional Differential Equations. New York: Wiley; 1993.

[30] Adomian G, Rach R. Modified adomian polynomials. Math Comput Model. 1996;24(11):39–46.

[31] Fatoorehchi H, Abolghasemi H. Improving the differential transform method: A novel technique to obtain the differential transforms of nonlinearities by the Adomian polynomials. Appl Math Model. 2013;37:6008–17.

[32] Wua G, Baleanu D, Luo W. Analysis of fractional nonlinear diffusion behaviors based on Adomian polynomials. Thermal Sci. 2017;21(2):813–7.

[33] Alfwzan W, Yao S, Allehiany FM, Ahmad S, Saifullah S, Inc M. Analysis of fractional non-linear tsunami shallow-water mathematical model with singular and non singular kernels. Results Phys. 2023;52:106707.

[34] Palais RS. A simple proof of the Banach contraction principle. J Fixed Point Theory Appl. 2007;2(2):221–3.

[35] Garcia-Falset J, Latrach K, Moreno-Gálvez E, Taoudi MA. Schaefer-Krasnoselskii fixed point theorems using a usual measure of weak noncompactness. J Differ Equ. 2012;252(5):3436–52.